

The High- z Quasar Hubble Diagram

Fulvio Melia¹

Department of Physics, the Applied Math Program, and Steward Observatory
The University of Arizona
Tucson, AZ 85721

E-mail: fmelia@email.arizona.edu

Abstract. Two recent discoveries have made it possible for us to begin using high- z quasars as standard candles to construct a Hubble Diagram (HD) at $z > 6$. These are (1) the recognition from reverberation mapping that a relationship exists between the optical/UV luminosity and the distance of line-emitting gas from the central ionizing source. Thus, together with a measurement of the velocity of the line-emitting gas, e.g., via the width of BLR lines, such as Mg II, a single observation can therefore in principle provide a determination of the black hole's mass; and (2) the identification of quasar ULAS J1120+0641 at $z = 7.085$, which has significantly extended the redshift range of these sources, providing essential leverage when fitting theoretical luminosity distances to the data. In this paper, we use the observed fluxes and Mg II line-widths of these sources to show that one may reasonably test the predicted high- z distance versus redshift relationship, and we assemble a sample of 20 currently available high- z quasars for this exercise. We find a good match between theory and observations, suggesting that a more complete, high-quality survey may indeed eventually produce an HD to complement the highly-detailed study already underway (e.g., with Type Ia SNe, GRBs, and cosmic chronometers) at lower redshifts. With the modest sample we have here, we show that the $R_h = ct$ Universe and Λ CDM both fit the data quite well, though the smaller number of free parameters in the former produces a more favorable outcome when we calculate likelihoods using the Akaike, Kullback, and Bayes Information Criteria. These three statistical tools result in similar probabilities, indicating that the $R_h = ct$ Universe is more likely than Λ CDM to be correct, by a ratio of about 85% to 15%.

¹John Woodruff Simpson Fellow.

Contents

1	Introduction	1
2	High-z Quasars as Standard Candles	3
3	The High-z Quasar Sample and Hubble Diagram	7
4	Theoretical Fits to the High-z Quasar HD	12
5	Discussion and Conclusions	15

1 Introduction

A powerful method of probing the cosmological expansion involves the acquisition of distance versus redshift data for sources whose absolute luminosity is accurately known. Plotting this information to produce (what is commonly referred to as) the Hubble Diagram (HD) then provides us with the expansion history of the Universe, and since the cosmic evolution depends critically on its constituents, measuring distances over a broad range of redshifts can in principle place meaningful constraints on assumed cosmological models. As is well known by now, it was this program that led to the discovery of dark energy through the use of Type Ia supernovae [1–5]. These events produce a relatively well-known luminosity, permitting them to function as reasonable standard candles, under the assumption that the power of both near and distant explosions can be standardized with the same luminosity versus color and light-curve shape relationships.

However, being reasonably sure that something other than (luminous and cold dark) matter and radiation must be present in the Universe is a far cry from understanding what dark energy is, or even knowing what its equation of state $p_{de} = w_{de}\rho_{de}$ must be, in terms of its pressure p_{de} , its energy density ρ_{de} , and the dimensionless parameter w_{de} that may or may not be changing with time. The standard model of cosmology (Λ CDM) posits that $w_{de} = -1$ at all times, the simplest assumption one can make based on Einstein’s cosmological constant Λ . This form of ρ_{de} may be a manifestation of vacuum energy, though its value would be at odds with the prediction from quantum mechanics.

But as impressive as the use of Type Ia SNe has been, several important limitations mitigate the overall impact of this work. Principal among these is the fact that even excellent space-based platforms such as SNAP have difficulty observing these events at redshifts > 1.8 . Since much of the interesting physics driving the evolution of the Universe occurred well before this epoch, we are therefore quite restricted in what we can learn from Type Ia SNe alone.

In addition, an incompatibility is now emerging between the use of the standard model to interpret Type Ia SNe and its application to other equally important observations, such as those of the cosmic chronometers [6] and the cosmic microwave background (CMB) [7, 8]. Growing tension between these measurements and the predictions of Λ CDM suggest that the standard model may not be providing an accurate representation of the cosmological expansion at high redshifts ($z \gg 2$). For example, the Wilkinson Microwave Anisotropy Probe (WMAP) [9] and *Planck* [10] have uncovered several anomalies in the full CMB sky

that appear to indicate possible new physics driving the growth of density fluctuations in the early Universe. These include an unusually low power at the largest scales and an apparent mutual alignment of the quadrupole and octopole moments, for which there appears to be no statistically significant correlation in Λ CDM. Their combined statistical significance is therefore equal to the product of their individual significances, suggesting that the simultaneous observation in the context of the standard model of the missing large-angle correlations with probability $< 0.1\%$ and a low- l multipole alignment with probability $\sim 4.9\%$ is likely at the $< 0.005\%$ level [11].

However, even at low redshifts, there are limitations to how well the Type Ia supernova data can be interpreted with an empirical model such as Λ CDM, because the data cannot be determined independently of the assumed cosmology—the supernova luminosities must be evaluated by optimizing at least 4 parameters simultaneously with those in the adopted model. This renders the data compliant to the underlying theory, so the model-dependent data reduction cannot be ignored in any comparative analysis between competing cosmologies. For example, we recently demonstrated that the Type Ia supernova HD in the best fit Λ CDM model is virtually indistinguishable from that in the $R_h = ct$ Universe [8, 12], over a redshift range extending all the way to $z \sim 6$ and beyond [7].

Having said this, there do exist model-independent data, such as the so-called cosmic chronometers [13], that one can use to test different expansion scenarios at low redshifts. In this approach, luminous red galaxies provide us with a method of measuring the universal expansion rate $H(z)$ in a model-independent way. However, our recent analysis of these data, comparing the standard model with the $R_h = ct$ Universe (discussed more extensively below), has shown that model selection tools, such as the Akaike, Kullback, and Bayes Information Criteria, disfavor Λ CDM [6]. On the basis of these data, the likelihood that the standard model is closer than $R_h = ct$ to the correct cosmology is less than $\sim 8 - 18\%$ (depending on which criterion one uses).

These are some of the reasons for seeking other kinds of standard candle to extend the HD to redshifts well beyond the Type Ia SNe range. An example of such a category of sources currently being studied for this purpose are gamma-ray bursts (GRBs) [14–16] which, like Type Ia SNe, are transient and believed to result from explosive stellar deaths (though in this case with a mass much bigger than that of the Sun). Recently, the *Swift* spacecraft has added considerably to the GRB database, from $z \sim 0$ all the way to $z \sim 6$. We ourselves have compiled an updated HD using GRBs detected in recent years, providing a means of testing cosmological models at intermediate redshifts, between the Type Ia SN range and $z > 6$ [17]. And here also we found that the standard model does not appear to be preferred by the observations. A comparative analysis between Λ CDM and the $R_h = ct$ Universe using the GRB data and the Akaike, Kullback, and Bayes Information Criteria suggests that the likelihood of Λ CDM being the correct cosmology instead of $R_h = ct$ is only $\sim 4 - 15\%$.

In this paper, we highlight several key recent discoveries that now allow us to suggest the use of high- z quasars as standard candles to construct a Hubble Diagram at redshifts beyond ~ 6 , but only under fairly stringent conditions. The first of these novel results is that the Mg II FWHM and UV luminosity of quasars beyond $z \sim 6$ appear to be correlated. Since reverberation mapping of their broad lines also reveals a relationship between the distance of the line-emitting gas from the central ionizing source and the optical/UV flux, these two features together can therefore yield a possibly useful measurement of the black-hole mass. In addition, estimates of their bolometric power using the F_{3000} flux density inferred from their fitted continuum suggest that the most luminous quasars at $z > 6$ may be accreting

near their Eddington limit, L_{Ed} [18, 19]. More importantly for the analysis we will carry out in this paper, the observed range of Eddington factors, λ_{Ed} , appears to be narrowing as $z \rightarrow 6-7$, centered on a value close to one. Here, $\lambda_{\text{Ed}} \equiv L_{\text{bol}}/L_{\text{Ed}}$, in terms of the bolometric (L_{bol}) and Eddington (L_{Ed}) luminosities. Thus, knowledge of their redshift and UV spectrum makes them potentially viable sources to use in order to construct a Hubble Diagram.

The second significant discovery that makes this idea viable was the detection of a luminous quasar at redshift $z = 7.085$ [20]. As we shall see, by extending the redshift coverage from the previous record around 6.4 to over 7, this single event has greatly improved the leverage attainable when fitting theoretical luminosity distances to the data. This is especially true in view of the growing realization that quasars tend to accrete closer to L_{Ed} as their redshift increases (see, e.g., ref. [21]). At the very least, there appears to be a transition from sub-Eddington to near Eddington-limited accretion as the redshift increases past ~ 6 [18, 19], though this inference may be due in part to selection effects, since it is primarily based on the observation of the most luminous sources at this redshift. As we shall see in subsequent sections, the inclusion of fainter quasars may somewhat mitigate this perceived general trend.

Any attempt at using supermassive black holes as standard candles comes with several important caveats, so the kind of analysis we are conducting here should not be viewed in isolation. The true benefit of this work will emerge only when the results are compared to efforts using Type Ia SNe at lower redshifts and, eventually, to the Hubble Diagram constructed from GRBs at intermediate redshifts. We will discuss some of the more obvious caveats in § 2 below, and then demonstrate how high- z quasars may be used to construct an HD in § 3. We will then compare this HD with two cosmological models in § 4, and discuss the results and present some conclusions in the final section of the paper.

2 High- z Quasars as Standard Candles

Reverberation mapping of the broad-line region in quasars produces a tight relationship between the distance R of the line-emitting gas from the central ionizing source, and the optical/UV luminosity, L_{UV} [22]. The form of this dependence,

$$R \propto L_{UV}^{0.5}, \quad (2.1)$$

is consistent with straightforward ionization models [23, 24]. Thus, the simultaneous measurement of the quasar’s luminosity and the velocity of its line-emitting gas, e.g., via the observation of its Doppler-broadened Mg II line, is sufficient, in principle, to determine the gravitational mass M of the central supermassive black hole [25]. However, one must be aware of the various sources of uncertainty still associated with these measurements, which limit the accuracy of the black-hole mass determination to $\approx 0.4 - 0.5$ dex [26]. Claims have been made that the accuracy may be as good as ≈ 0.3 dex [27], though these may be unrealistic (see also refs. [28–30] for a review of the reliability and accuracy of this method).

This limited uncertainty is important because the use of high- z quasars as standard candles relies quite critically on how accurately M can be determined. If high-quality line and continuum measurements are available, one can use the relationship [31]

$$\log M = 6.86 + 2 \log \frac{\text{FWHM}(\text{MgII})}{1,000 \text{ km s}^{-1}} + 0.5 \log \frac{L_{3000}}{10^{44} \text{ ergs s}^{-1}}, \quad (2.2)$$

in terms of the Mg II line width, $\text{FWHM}(\text{Mg II})$, and the luminosity L_{3000} at rest-frame 3000 Å. This mass-scaling relationship was obtained using several thousand high-quality spectra from the SDSS DR3 quasar sample [32], with a calibration to the $\text{H}\beta$ and C IV relations. The scaling law was applied to the subset of the DR3 quasar sample used to establish the luminosity [33] and black-hole mass [34] functions. Equation (2.2) has been employed quite effectively to measure quasar masses [18] in the analysis of nine Canada-France High- z Quasar Survey (CFHQS) sources, and an additional eight SDSS sources with near-IR Mg II spectroscopy of sufficient quality to match that of the CFHQS sample. The SDSS quasars were originally reported in refs. [35–37]. All 17 of these sources, together with several others from ref. [19], and the newest quasar ULAS J1120+0641 at $z = 7.085$ [20], are included in Table 1 below.

The F_{3000} flux density is measurable to an accuracy of about 10% [18]. The FWHM is measurable to a corresponding accuracy of about 15%. Thus, determining the black hole masses by inserting the extreme values of L_{3000} and the FWHM (based on their rms uncertainties) into the above equation yields a mass estimate uncertain by a factor of several (i.e., the aforementioned $\approx 0.4 - 0.5$ dex; [28, 30]). This is evident from the range of masses quoted for each source listed in Table 1. As we shall show below, the measured values of $\text{FWHM}(\text{MgII})$ and L_{3000} may be used for tests of cosmological models without actually calculating the black-hole mass M itself, though the uncertainty in these quantities carries through to a determination of the HD constructed from them.

The luminosities and masses inferred from the measured fluxes, and the luminosity distance inferred from the observed redshift, all depend on the assumed cosmology. Fortunately, we will not need to use these inferred quantities to construct the HD, but show their values here for illustrative purposes. The entries listed in Table 1 correspond to a Λ CDM model with a Hubble constant $H_0 = 70 \text{ km s}^{-1} \text{ Mpc}^{-1}$, and a scaled matter density $\Omega_m = 0.28$, where $\Omega_m \equiv \rho_m/\rho_c$. The critical density $\rho_c \equiv 3c^2 H_0^2/(8\pi G)$ is determined under the assumption that the Universe is flat, so the total scaled energy density $\Omega \equiv \Omega_m + \Omega_r + \Omega_\Lambda$ equals 1. The other quantities in this expression are the corresponding radiation ($\Omega_r \equiv \rho_r/\rho_c$) and dark energy ($\Omega_\Lambda \equiv \rho_\Lambda/\rho_c$) densities.

The values of F_{3000} were derived from the fitted continuum, and their uncertainties include 10% added in quadrature to account for the absolute flux calibration uncertainty. The monochromatic luminosity is only a fraction of the total power produced by the quasar, so a bolometric correction η must be applied to find its total luminosity, L_{bol} ($\equiv \eta L_{3000}$; this is shown for Λ CDM in the fifth column of Table 1). These values were obtained from L_{3000} using a bolometric factor $\eta = 6.0$ [38, 39], though the estimation of L_{bol} from a single monochromatic luminosity can be quite uncertain for individual objects, given the diversity of quasar spectral energy distributions (SEDs) (see, e.g., the cautionary discussions in [38]).

The SEDs in ref. [38] update the mean SED from ref. [40], often used previously to derive bolometric luminosities and accretion rates. These newer SEDs were constructed from 259 SDSS quasars, combining SDSS magnitudes and *Sptizer* IRAC flux densities, though with some “gap repair” in other bands for which some sources have no measurements. The quasar spectra were also corrected for host galaxy contamination, using scaling relationships among host bulge luminosity, bulge mass, black-hole mass, and Eddington luminosity, to estimate the contribution of host galaxy light to the quasar SEDs [41, 42]. The quasar luminosity versus host luminosity relationship at optical frequencies provides a reasonable estimate of the host galaxy contribution, under the assumption that the quasars are emitting at their Eddington limit.

Table 1. High- z Quasars

Name	z	M^\dagger $10^8 M_\odot$	FWHM (Mg II) km s^{-1}	L_{bol}^\dagger $10^{45} \text{ ergs s}^{-1}$	$d_L^{\Lambda\text{CDM}^\dagger}$ Gly	Ref.
ULAS J1120+0641	7.085	13–35	3800 ± 200	252	227.21	[20]
CFHQS J0210-0456	6.438	0.4–1.35	1300 ± 350	22–28	203.32	[18]
SDSS J1148+5251	6.419	44–87	6000 ± 850	360	202.62	[18]
CFHQS J2329-0301	6.417	2.1–2.9	2020 ± 110	37–47	202.55	[18]
SDSS J1030+0524	6.310	12–24	3600 ± 100	180	198.63	[36]
CFHQS J0050+3445	6.253	22–31	4360 ± 270	185–226	196.54	[18]
SDSS J1623+3112	6.250	11–21	3600 ± 411	171	196.43	[35]
SDSS J1048 + 4637	6.198	25–62	3366 ± 532	304	194.53	[19]
CFHQS J0221-0802	6.161	2.3–14.5	3680 ± 1500	27–33	193.18	[18]
CFHQS J2229+1457	6.152	0.7–1.9	1440 ± 330	32–40	192.85	[18]
CFHQS J1509-1749	6.121	27–33	4420 ± 130	238–290	191.72	[18]
CFHQS J2100-1715	6.087	6.9–12.3	3610 ± 420	53–65	190.47	[18]
SDSS J0303-0019	6.080	2.6–5	2300 ± 125	53	190.22	[37]
SDSS J0353 + 0104	6.072	9–22	3682 ± 281	146	189.93	[19]
SDSS J0842 + 1218	6.069	11–27	3931 ± 257	155	189.82	[19]
SDSS J1630 + 4012	6.058	6–14	3366 ± 533	94	189.42	[19]
CFHQS J1641+3755	6.047	1.6–3.4	1740 ± 190	64–80	189.02	[18]
SDSS J1306 + 0356	6.020	19–36	4500 ± 160	192	188.03	[36]
CFHQS J0055+0146	5.983	1.7–3.3	2040 ± 280	34–42	186.68	[18]
SDSS J1411+1217	5.950	6–10	2400 ± 150	240	185.48	[36]

† Assumed parameters: $H_0 = 70 \text{ km s}^{-1} \text{ Mpc}^{-1}$, $\Omega_m = 0.28$, and $\Omega \equiv \Omega_m + \Omega_r + \Omega_\Lambda = 1$.

An important caveat with this work is that in order to construct mean SEDs, the flux densities of each individual object can be compared or combined with those of other quasars in the sample by adopting a particular cosmology. Thus, the process of obtaining an average value of η is not entirely free of the presumed background expansion scenario. Insofar as comparing $R_h = ct$ with ΛCDM using the high- z quasar sample is concerned, this is not a serious problem because, as we shall see, the concordance ΛCDM model essentially replicates the dynamics of $R_h = ct$, so that if one were to use the latter to construct the average quasar SED [33, 38], the outcome would be very close to what they obtained using a standard flat cosmology with $H_0 = 70 \text{ km s}^{-1} \text{ Mpc}^{-1}$, $\Omega_m = 0.3$, and $\Omega_\Lambda = 0.7$.

A second caveat is that parts of the SED, such as the MIR, change for different quasar properties. Though the shape of the MIR is very similar for optically blue and optically red quasars, there are significant differences between the most and least optically luminous quasars in their sample. The optically luminous quasars are much brighter in the $4 \mu\text{m}$ region than the least optically luminous objects, which is probably due to physical effects, such as orientation and dust temperature.

A final caveat is that bolometric corrections and bolometric luminosities determined by

summing up all of the observed flux are in reality line-of-sight values that assume quasars are emitting isotropically, whereas this is known not to be completely correct. All in all, computing a bolometric luminosity from an optical luminosity by assuming a single mean quasar SED may lead to errors as large as $\sim 50\%$ [38].

These caveats notwithstanding, all of the SEDs constructed in refs. [38, 39] result in a consistent bolometric correction at $3,000 \text{ \AA}$. Taking the bolometric luminosity to encompass all of the emission from 100 \mu m to 10 keV , η at this wavelength ranges from about 5 to 6 for all of the quasar properties (see figs. 12 and 13 in ref. [38]). In fact, in the $3,000 \text{ \AA}$ rest frame, the differences in the composite SEDs for all the quasar sub-classes are relatively small. This therefore appears to be a robust choice of wavelength for converting monochromatic luminosity to bolometric luminosity, because the minimum in this region is due to a relative minimum in the combination of host galaxy contamination in the near-IR and dust extinction in the UV. Unfortunately, there does not appear to be any strong trend between the bolometric correction and color or luminosity, so it is difficult to know when to apply anything other than the mean bolometric correction, which we will do throughout this work.

The acquisition of some of the data quoted in Table 1 was made possible by the correlation seen between the Mg II FWHM and L_{3000} . This constraint is even more interesting in view of its observed absence at lower redshifts [43, 44], which may be attributed to the fact that the nearby quasars are accreting at a very wide range of sub-Eddington rates [18]. Thus, the emergence of this correlation above $z \sim 6$ is evidence that the distant sources may be accreting within a narrower range of Eddington fractions. Indeed, these results are consistent with most of the high- z quasars accreting near Eddington values.¹

Other (more circumstantial) evidence that the high- z quasars are accreting at near-Eddington rates is based on the maximum black-hole mass observed in the local Universe [44]. Only a few black-hole masses exceeding $10^{10} M_{\odot}$ have thus far been detected [45, 46], even after the peak of quasar activity at $1 < z < 3$. Yet most high- z quasars accreting below L_{Ed} would have to be more massive than $10^{10} M_{\odot}$ in order to produce the fluxes measured at Earth. In principle, some of the CFHQS quasars have more moderate luminosities, so they could be accreting at sub-Eddington rates. But even in this case [18], the lower luminosities are due to smaller masses (closer to $\sim 10^8 M_{\odot}$), rather than to lower accretion rates.

The conclusion from this meticulous work is that the moderate to high-luminosity quasars at $z > 6$ appear to be accreting close to their Eddington rate. This may not be true for the fainter sources, which may be accreting at a broad range of Eddington ratios even for high redshifts. As a result, there may be a practical limit to the number of suitable high- z objects that are useful as standard candles. This caveat notwithstanding, there is some evidence that the mean Eddington ratio does increase with redshift (see, e.g., figure 19 in ref. [21]). As we shall see shortly, this is quite useful in itself for constructing a Hubble Diagram but, more importantly, the transition from sub-Eddington to near-Eddington accretion rates across $z \sim 6$, and the accumulation of circumstantial evidence we have just described, point to a narrowing in the range of Eddington factors above $z \sim 6$, with no further evidence of evolution in their distribution function $\phi(\lambda_{\text{Ed}})$ towards higher redshifts.

The high- z quasars appear to be in the exponential buildup of their mass, and have not yet reached the later phase of quasar activity where the accretion rate declines to the sub-Eddington values we see locally. For this principal reason, we suggest that high- z quasars with

¹The fact that the tight correlation between the Mg II FWHM and L_{3000} emerges only for $z > 6$ is one of the principal reasons why the sample we must use to construct the high- z quasar HD cannot include AGNs and quasars at lower redshifts.

a reasonable determination of their F_{3000} flux density and Mg II line-widths may therefore be used as reasonable sources to generate a Hubble Diagram at $z > 6$, well beyond the reach of Type Ia SNe and (probably) also beyond the redshift range where most GRBs will be detected.

We should also point out an interesting alternative suggestion to use super-Eddington accreting quasars as cosmological standards [47], based on the realization that photon trapping [48] in some sources affects the total emitted radiation and results in a saturated luminosity for a given black-hole mass, which can therefore be used to deduce cosmological distances. In these black-hole systems, the X-ray emission is linked to the optical-UV spectrum of the accretion disk, and so in principle, may be identified through hard X-ray observations. Thus far, however, the best group of AGNs where such processes have been studied are narrow line Seyfert 1 galaxies, predominantly at redshifts $z \lesssim 0.3$. It may be difficult to use this technique to extrapolate to redshifts > 6 , the principal aim of this paper.

3 The High- z Quasar Sample and Hubble Diagram

The entries shown in Table 1 were obtained by pre-assuming a Λ CDM model with concordance parameter values. These high- z quasars represent the majority of cases for which a reasonable estimate of mass has been made to date. However, for obvious reasons, this is not an ideal approach to take when attempting to use the high- z quasar HD to test competing cosmological expansion scenarios. In principle, one could recalibrate the data for each assumed model and then check for consistency *a posteriori*. Unfortunately, this appears to be an essential ingredient with any attempt at using Type Ia SNe for this purpose, since the data are themselves characterized by four so-called nuisance parameters that need to be optimized along with the pre-assumed model [1–3, 7]. Fortunately, we do not need to follow this procedure here, since the high- z quasar data may be used without pre-assuming a cosmological expansion, but only under the (reasonable) assumption that the $z > 6$ sources are indeed accreting within a narrow range of Eddington factors, presumably centered on a value close to one and, most importantly, that their Eddington luminosity function $\phi(\lambda_{\text{Ed}})$ is not changing with redshift.

We will first examine whether the idea of constructing a high- z HD can lead to useful results, given the various uncertainties associated with the measurements themselves. In the expression for λ_{Ed} , the Eddington rate is defined from the maximum luminosity attainable due to outward radiation pressure acting on highly ionized infalling material [49]. This power depends somewhat on the gas composition, but for hydrogen plasma is given as $L_{\text{Ed}} \approx 1.3 \times 10^{38} (M/M_{\odot}) \text{ ergs s}^{-1}$, in terms of the accretor’s mass, M . For a more general composition, in which the electron’s mean atomic weight is μ_e , this expression becomes $L_{\text{Ed}} \approx 1.3 \times 10^{38} \mu_e (M/M_{\odot}) \text{ ergs s}^{-1}$. (For example, $\mu_e = 2$ when the accreting plasma is pure helium.)

The distribution of Eddington ratios λ_{Ed} in quasars is an important probe into the quasar activity and black-hole growth. Lower redshift studies [26, 50] show that the λ_{Ed} distribution up to $z = 4$ in luminosity and redshift bins is a lognormal that shifts to higher λ_{Ed} and narrows for the higher luminosities. The most luminous quasars (i.e., $L_{\text{bol}} > 10^{47} \text{ ergs s}^{-1}$) at $2 < z < 3$ have a typical $\lambda_{\text{Ed}} = 0.25$ and dispersion of 0.23 dex [26]. The latest results (see, e.g., figure 6 in ref. [18]) show that the λ_{Ed} distribution at $z = 6$ can also be approximated by a lognormal, though here with peak $\lambda_{\text{Ed}} = 1.07$, and dispersion 0.28 dex. The available evidence, though mostly circumstantial, suggests that the λ_{Ed} distribution at higher redshifts remains centered near one, as we have described above.

Table 2. Measured (Dimensionless) Luminosity Distances

Name	z	FWHM (Mg II) km s ⁻¹	$F_\nu(3000 \text{ \AA})$ 10 ⁻²⁹ ergs/cm ² /s/Hz	Δ_L	Ref.
ULAS J1120+0641	7.085	3800 ± 200	5.82 ± 0.43	6.0 ± 0.9	[20]
CFHQS J0210-0456	6.438	1300 ± 350	0.67 ± 0.08	2.1 ± 1.5	[18]
SDSS J1148+5251	6.419	6000 ± 850	12.7 ± 0.20	10.1 ± 3.1	[18]
CFHQS J2329-0301	6.417	2020 ± 110	1.13 ± 0.13	3.8 ± 0.7	[18]
SDSS J1030+0524	6.310	3600 ± 100	5.64 ± 0.09	5.5 ± 0.3	[36]
CFHQS J0050+3445	6.253	4360 ± 270	6.42 ± 0.64	7.5 ± 1.4	[18]
SDSS J1623+3112	6.250	3600 ± 411	5.43 ± 0.15	5.6 ± 1.4	[35]
SDSS J1048 + 4637	6.198	3366 ± 532	12.7 ± 0.10	3.2 ± 1.1	[19]
CFHQS J0221-0802	6.161	3680 ± 1500	5.45 ± 0.55	5.8 ± 5.8	[18]
CFHQS J2229+1457	6.152	1440 ± 330	1.02 ± 0.10	2.1 ± 1.2	[18]
CFHQS J1509-1749	6.121	4420 ± 130	7.54 ± 0.75	7.1 ± 0.9	[18]
CFHQS J2100-1715	6.087	3610 ± 420	1.69 ± 0.17	10.0 ± 3.1	[18]
SDSS J0303-0019	6.080	2300 ± 125	1.8 ± 0.03	3.9 ± 0.5	[37]
SDSS J0353 + 0104	6.072	3682 ± 281	6.48 ± 0.3	5.3 ± 1.0	[19]
SDSS J0842 + 1218	6.069	3931 ± 257	7.14 ± 0.36	5.8 ± 1.0	[19]
SDSS J1630 + 4012	6.058	3366 ± 533	4.38 ± 0.9	5.4 ± 2.8	[19]
CFHQS J1641+3755	6.047	1740 ± 190	2.09 ± 0.23	2.1 ± 0.6	[18]
SDSS J1306 + 0356	6.020	4500 ± 160	5.91 ± 0.12	8.3 ± 0.7	[36]
CFHQS J0055+0146	5.983	2040 ± 280	1.12 ± 0.12	3.9 ± 1.5	[18]
SDSS J1411+1217	5.950	2400 ± 150	9.09 ± 0.18	1.9 ± 0.3	[36]

At $z = 6$, the peak of the distribution is therefore four times higher than for the most luminous quasars at $2 < z < 3$. Indeed, as we noted in the previous section, the typical quasar at $z = 6$ appears to be accreting right at the Eddington limit, with only a narrow distribution in λ_{Ed} . But the width of this distribution is not negligible and an important question that needs to be answered is whether one may still use the high- z quasars as standard candles in spite of this spread. To circumvent this problem, we will average over $\phi(\lambda_{\text{Ed}})$ at each sampled redshift. As we shall see, the benefit of this method is that it avoids the inevitable scatter produced by the spread in individual λ_{Ed} values.

Let us now quickly review the newly defined quantities and the assumptions we have made, while deriving an expression for the luminosity distance in terms of the observable parameters. Beginning with Equation (2.2) and the definition of the Eddington luminosity, we get

$$\frac{L_{\text{Ed}}}{1.3 \times 10^{38} \text{ ergs s}^{-1} \mu_e} = 10^{6.86} \left(\frac{\text{FWHM}(\text{MgII})}{1,000 \text{ km s}^{-1}} \right)^2 \times \left(\frac{L_{3000}}{10^{44} \text{ ergs s}^{-1}} \right)^{1/2}, \quad (3.1)$$

where FWHM(MgII) is the Mg II line width at half-maximum, L_{3000} is the luminosity at rest-

frame 3000 \AA , and μ_e is the electron's mean atomic weight ($= 1.17$ for cosmic abundances; see below), which we assume does not change over the redshift range of interest ($z < 1000$). Thus, in terms of the bolometric factor $\eta \equiv L/L_{3000}$ (assumed to have the value 6) and Eddington factor $\lambda_{\text{Ed}} \equiv L/L_{\text{Ed}}$ (presumably of order 1), this becomes

$$\frac{\eta L_{3000}}{1.3 \times 10^{38} \text{ ergs s}^{-1} \mu_e \lambda_{\text{Ed}}} = 10^{6.86} \left(\frac{\text{FWHM}(\text{MgII})}{1,000 \text{ km s}^{-1}} \right)^2 \times \left(\frac{L_{3000}}{10^{44} \text{ ergs s}^{-1}} \right)^{1/2}. \quad (3.2)$$

Finally, replacing L_{3000} with the expression

$$L_\lambda = 4\pi c d_L^2 \frac{F_\nu}{\lambda}, \quad (3.3)$$

where d_L is the luminosity distance and $\nu = c/\lambda$, we arrive at

$$d_L = (55.0 \text{ Glyr}) \lambda_{\text{Ed}} \left(\frac{\mu_e}{1.17} \right) \left(\frac{\eta}{6} \right)^{-1} \left(\frac{\text{FWHM}}{1,000 \text{ km s}^{-1}} \right)^2 \times \left(\frac{F_\nu}{10^{-29} \text{ ergs cm}^{-2} \text{ s}^{-1} \text{ Hz}^{-1}} \right)^{-1/2}. \quad (3.4)$$

We will write this equation as

$$d_L(z) = \lambda_{\text{Ed}} K \Delta_L(z), \quad (3.5)$$

where

$$\Delta_L(z) \equiv \left(\frac{\text{FWHM}}{1,000 \text{ km s}^{-1}} \right)^2 \left(\frac{F_\nu}{10^{-29} \text{ ergs cm}^{-2} \text{ s}^{-1} \text{ Hz}^{-1}} \right)^{-1/2}, \quad (3.6)$$

and the constant K incorporates all of the other factors appearing in Equation (3.4), except for λ_{Ed} . That is,

$$K \equiv (55.0 \text{ Glyr}) \left(\frac{\mu_e}{1.17} \right) \left(\frac{\eta}{6} \right)^{-1}. \quad (3.7)$$

In these expressions, the mean molecular weight per electron,

$$\mu_e \approx \frac{2}{1 + X_{\text{H}}}, \quad (3.8)$$

has been scaled to the value, 1.17, corresponding to cosmic abundances, i.e., a fraction $X_{\text{H}} \approx 0.7$ of Hydrogen by mass.

Expressed in this fashion, d_L and Δ_L are independent of any cosmological model, though in principle, all three quantities μ_e , η , and λ_{Ed} may change from quasar to quasar. But since μ_e depends primarily on the helium to hydrogen abundance ratio, which changed very little since big bang nucleosynthesis, and η appears to be independent of source under a wide range of conditions (see previous section), one may reasonably expect these two parameters (and therefore K) to be nearly constant.

Insofar as λ_{Ed} is concerned, the data suggest a compression of Eddington factors with an average $\langle \lambda_{\text{Ed}} \rangle \sim 1.07$ for $z \sim 6 - 7$. Nonetheless, one cannot ignore the fact that the distribution $\phi(\lambda_{\text{Ed}})$, normalized such that

$$\int \phi(\lambda_{\text{Ed}}) d\lambda_{\text{Ed}} = 1, \quad (3.9)$$

Table 3. Binned Sample

Redshift	$\langle \Delta_L \rangle$	σ
5.95 – 6.05	4.1	2.6
6.05 – 6.15	6.3	1.9
6.15 – 6.25	3.7	1.6
6.25 – 6.35	6.2	0.9
6.35 – 6.45	5.3	3.4
7.05 – 7.15	6.0	0.9 [†]

[†]Calculated from the standard deviation of the individual source (ULAS J1120+0641) in this bin. For comparison, we also consider an outcome based on the use of a sample-averaged standard deviation (i.e., $\sigma = 1.9$) for the $z = 7.05 - 7.15$ bin.

is lognormal with a dispersion 0.28 dex. So even though the average $\langle \lambda_{\text{Ed}} \rangle$ is close to 1 and apparently independent of redshift for $z > 6$, the bolometric luminosity of individual quasars may deviate from their Eddington limit by factors of ~ 2 . Thus, instead of constructing the HD from individual sources, we can avoid the consequent scatter produced by this spread in λ_{Ed} by simply averaging over the Eddington factor at each sampled redshift.

In principle, ϕ may also depend on z , and the data do show that this is the case for $z \leq 6$, as we have noted earlier. But since $\langle \lambda_{\text{Ed}} \rangle$ levels off at ~ 1 for $z \sim 6 - 7$, we will assume that in this range ϕ is only a function of λ_{Ed} . Within a small redshift bin $\Delta z = z_2 - z_1$ at $z = (z_1 + z_2)/2$, we may then write

$$\langle d_L(z) \rangle = K \langle \lambda_{\text{Ed}} \rangle \langle \Delta_L(z) \rangle_{\text{sample}} , \quad (3.10)$$

where

$$\langle \lambda_{\text{Ed}} \rangle \equiv \int d\lambda_{\text{Ed}} \phi(\lambda_{\text{Ed}}) \lambda_{\text{Ed}} , \quad (3.11)$$

and $\langle \Delta_L(z) \rangle_{\text{sample}}$ is the sample average in that bin. The advantage of using these averages over individual sources is rather clear. If all of the assumptions and inferences we have made leading up to this equation are valid, the expectation is that both K and $\langle \lambda_{\text{Ed}} \rangle$ (~ 1) should be constant. Thus, by finding the sample average $\langle \Delta_L(z) \rangle_{\text{sample}}$ in each bin Δz , one may infer the average luminosity distance $\langle d_L(z) \rangle$, and use it to construct the high- z quasar HD to test competing cosmological models.

The individual dimensionless source distances Δ_L measured in this way are listed in Table 2, together with the flux densities F_ν and Mg II line-widths used to calculate them. With the catalog of 20 sources from Table 1, a reasonable bin size is $\Delta z = 0.1$, which one may use to calculate the sample-averaged values $\langle \Delta_L(z) \rangle$ quoted in Table 3. The third column shows the population standard deviation for each bin, except for $z = 7.05 - 7.15$. Since this bin contains only one source, the quoted standard deviation is simply that of ULAS

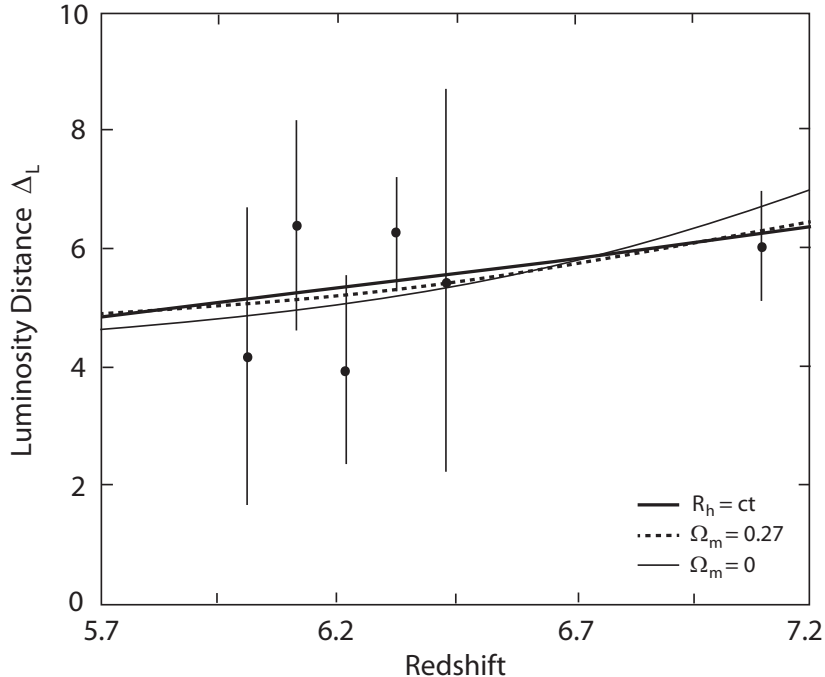


Figure 1. Sample-averaged (dimensionless) luminosity distance $\langle \Delta_L \rangle$ from Table 3. The solid curve gives the corresponding luminosity distance $d_L^{R_h=ct}$ in the $R_h = ct$ Universe, while the best fit Λ CDM model, with $\Omega_m = 0.27$ and $w_{de} = -1$, is shown as a dashed line. For comparison, we also show a Λ CDM model with $\Omega_m = 0$ (thin solid line), to highlight the dependence of these redshift-distance relationships on the parameters. The curves shown here all correspond to the values $K = 40.3$ Gyr, $\langle \lambda_{Ed} \rangle = 1$, and $H_0 = 70.0$ km s $^{-1}$ Mpc $^{-1}$. To produce these fits, we need 3 parameters for Λ CDM and 1 for $R_h = ct$. Therefore, the reduced χ_{dof}^2 for these curves is 0.76 for the optimized Λ CDM, 0.88 for Λ CDM with $\Omega_m = 0$, and 0.48 for $R_h = ct$.

J1120+0641 itself. However, in order to ensure that this particular source does not unduly influence the optimization of the fits relative to the other bins, in our analysis below we will also consider an outcome based on the use of a sample-averaged standard deviation for the highest redshift bin.

The binned data in Table 3 are plotted in figure 1, together with the theoretical fits we will discuss in the next section. A quick estimate of the luminosity distance calculated from Equation (3.5), using the scaling in Equation (3.7), shows that with these values our “measured” distance $d_L(z)$ appears to over-estimate the luminosity distance one would expect in the standard model (see Table 1) by $\sim 20 - 40\%$. There are several possible reasons for this. One of them is that we have carefully included the dependence of L_{Ed} on μ_e , which was ignored in earlier applications [18]. Unfortunately, we cannot know for sure what abundances characterize the medium surrounding these sources, but the introduction of μ_e into these expressions produces at least a $\sim 17\%$ difference from previously calculated λ_{Ed} values. Secondly, as we have alluded to previously, there appears to be at least a $\sim 20\%$ uncertainty in the value of η . So, for example, if we were to use the scaling $K = (40.3 \text{ Gyr}) (\mu_e/1.0)(\eta/7)^{-1}$, instead of Equation (3.7), the distances measured with Equation (3.5) would be right in line with the luminosity distances quoted for the standard model in Table 1.

Fortunately, these uncertainties do not affect the shape of our $\langle d_L(z) \rangle$ curve calculated

from Equation (3.10). All Friedmann-Robertson-Walker metrics have a luminosity distance proportional to c/H (see below), so our current imprecise knowledge of these factors directly affects the value of the Hubble constant that we could infer from fits to the high- z quasar data. Since the overall uncertainty in K appears to be $\sim 20-40\%$, it therefore does not make sense to worry about optimizing the value of H in these fits, since measurements of H using other techniques are much more reliable. Thus, until μ_e and η are known more precisely, we will compare how well competing cosmologies do in fitting the high- z quasar HD by concentrating solely on the shape of the $\langle d_L(z) \rangle$ or, equivalently, the $\langle \Delta_L(z) \rangle$, distributions in figure 1. But to illustrate how the value of H_0 would have impacted the fits to the quasar data, we show in figures 2 and 3 the luminosity distance versus redshift for the data in figure 1, and three curves: (a) $H_0 = 60 \text{ km s}^{-1} \text{ Mpc}^{-1}$, (b) $H_0 = 69.32 \text{ km s}^{-1} \text{ Mpc}^{-1}$ (the Planck best-fit value; see Ade et al. [10]), and (c) $H_0 = 80 \text{ km s}^{-1} \text{ Mpc}^{-1}$.

4 Theoretical Fits to the High- z Quasar HD

To demonstrate the future potential for using the high- z quasar HD in order to distinguish between competing cosmologies, we will here compare the entries in Table 3 with two different expansion scenarios: Λ CDM (with its three free parameters, H_0 , Ω_m , and the dark-energy equation of state w_{de}) and the $R_h = ct$ Universe, which has only one free parameter, the Hubble constant H_0 (though H_0 will not be optimized here for either cosmology; see §3 above). If we choose $w_{de} = -1$ (thus reducing the number of free parameters to 2), it is not difficult to show that in Λ CDM the expected luminosity distance is [7]

$$d_L^{\Lambda\text{CDM}} = \frac{c}{H_0}(1+z) \int_{\frac{1}{1+z}}^1 \frac{du}{\sqrt{\Omega_r + u\Omega_m + u^4\Omega_\Lambda}}, \quad (4.1)$$

in terms of the scaled radiation (Ω_r), matter (Ω_m), and dark-energy (Ω_Λ) densities.

The $R_h = ct$ cosmology is still not widely known, so we will begin by introducing some of its principal features. One way of looking at the expansion of the Universe is to guess its constituents and their equations of state and then solve the dynamics equations to determine the expansion rate as a function of time. This is the approach taken by Λ CDM. A second—though not mutually exclusive—way is to use symmetry arguments and our knowledge of the properties of a gravitational horizon in general relativity (GR) to determine the spacetime curvature, and thereby the expansion rate, strictly from just the value of the total energy density ρ and the implied geometry, without necessarily having to worry about the specifics of the constituents that make up the density itself. This is the approach adopted by $R_h = ct$. The constituents of the Universe must then partition themselves in such a way as to satisfy that expansion rate. In other words, what matters is ρ and the overall equation of state $p = w\rho$, in terms of the total pressure p and total energy density ρ . In $R_h = ct$, it is the aforementioned symmetries and other constraints from GR that uniquely fix w to have the value $-1/3$ [8, 12].

The $R_h = ct$ Universe is a Friedmann-Robertson-Walker (FRW) cosmology in which Weyl’s postulate takes on a more important role than has been considered before. Most workers assume that Weyl’s postulate is already incorporated into all FRW metrics, but actually it is only partially incorporated. Simply stated, Weyl’s postulate says that any proper distance $R(t)$ must be the product of a universal expansion factor $a(t)$ and an unchanging co-moving radius r , such that $R(t) = a(t)r$. The conventional way of writing an FRW metric

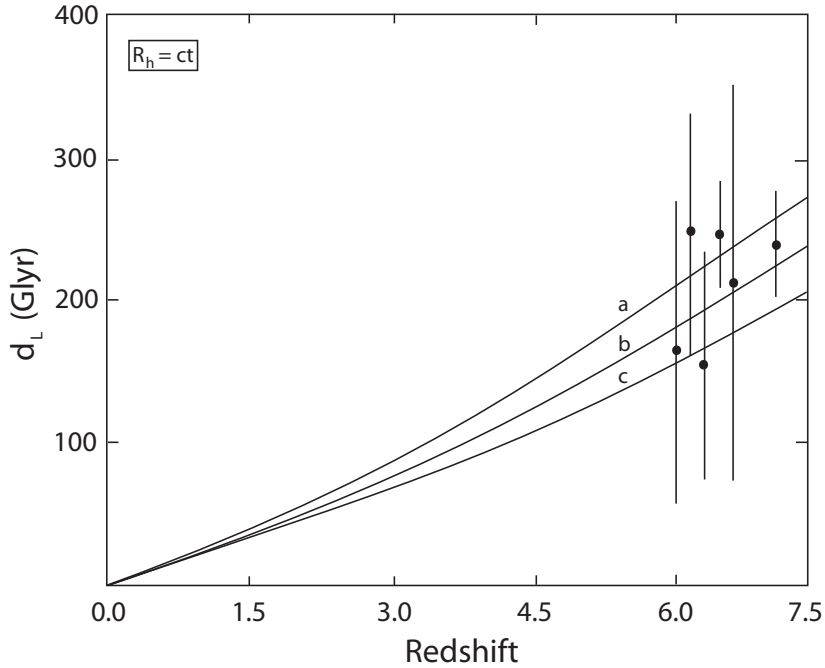


Figure 2. The luminosity distance versus redshift for the same data shown in figure 1. The curves illustrate the dependence of the fit on the Hubble constant and are for the $R_h = ct$ Universe with three different values of H_0 : (a) $60 \text{ km s}^{-1} \text{ Mpc}^{-1}$, (b) $69.32 \text{ km s}^{-1} \text{ Mpc}^{-1}$ (the Planck best-fit value; see Ade et al. 2013), and (c) $80 \text{ km s}^{-1} \text{ Mpc}^{-1}$. The other parameters are $K = 40.3 \text{ Glyr}$ and $\langle \lambda_{\text{Ed}} \rangle = 1$.

adopts this coordinate definition, along with the cosmic time t , which is actually the observer’s proper time at his/her location. But what is often overlooked is the fact that the gravitational radius, $R_h \equiv c/H$, which has the same definition as the Schwarzschild radius, and actually coincides with the better known Hubble radius, is in fact itself a proper distance too [51]. And when one forces this radius to comply with Weyl’s postulate, there is only one possible choice for $a(t)$, i.e., $a(t) = (t/t_0)$, where t_0 is the current age of the Universe. This also leads to the result that the gravitational radius must be receding from us at speed c , which is in fact how the Hubble radius was defined in the first place, even before it was recognized as another manifestation of the gravitational horizon.

The fact that $p = -\rho/3$ in $R_h = ct$ means that quantities, such as the luminosity distance and the redshift-dependent Hubble constant $H(z)$, take on very simple, analytical forms [6, 7]:

$$d_L^{R_h=ct} = \frac{c}{H_0}(1+z) \ln(1+z), \quad (4.2)$$

and

$$H(z) = H_0(1+z). \quad (4.3)$$

Yet even though these functional forms are quite different from their Λ CDM counterparts, in the end, regardless of how Λ CDM and $R_h = ct$ handle ρ and p , they must both account for the same cosmological data. And there is now growing evidence that Λ CDM functions as a reasonable approximation to $R_h = ct$ in some redshift ranges, but apparently not in others, as discussed in the introduction. Interestingly, we will find that here too, with the

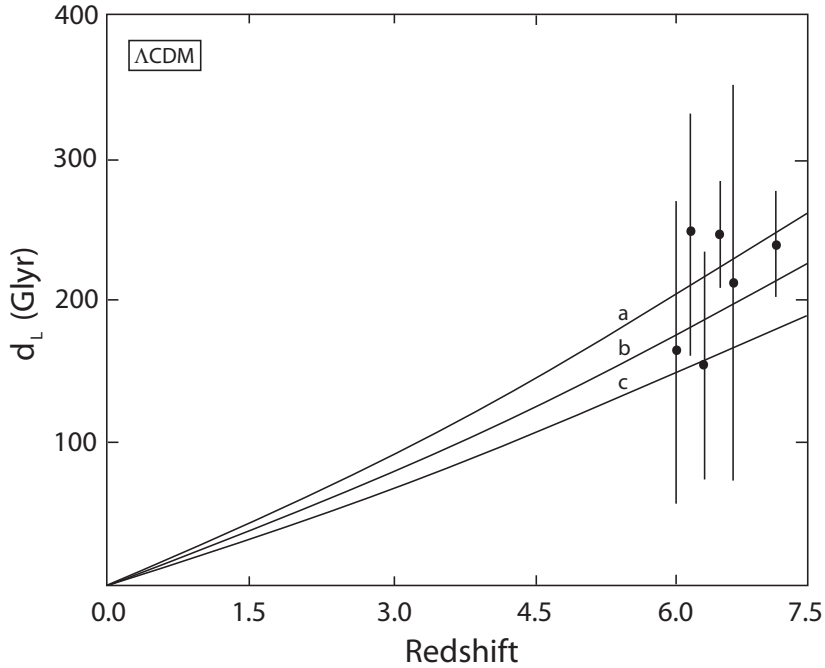


Figure 3. Same as figure 2, except now for Λ CDM. In addition to the parameters $K = 40.3$ Glyr and $\langle \lambda_{\text{Ed}} \rangle = 1$, these curves also assume $\Omega_m = 0.29$ (again from the Planck best fit), and a dark-energy equation-of-state $w_{de} \equiv w_\Lambda = -1$.

high- z quasar HD, the optimized Λ CDM model that best fits the data comes as close as its parametrization allows it to the $R_h = ct$ curve.

The theoretical curves that best fit the data are shown in figure 1, for both the $R_h = ct$ Universe (solid, thick line) and Λ CDM (dashed line). To gauge the dependence of these results on the parameters, we also show the curve corresponding to Λ CDM with $\Omega_m = 0$. (The more general dependence of the Λ CDM fit on the value of Ω_m is shown in figure 4.) With only one free parameter, the χ^2_{dof} for $R_h = ct$ is 0.48, compared with 0.76 and 0.88 for the Λ CDM fits. Based solely on their χ^2 -values, one would therefore conclude that all three models provide reasonable fits to the high- z quasar HD. However, model selection tools strongly favor models with fewer degrees of freedom, so the likelihood of any of these models being closest to the correct cosmology is different for the three cases (see §5 below).

Note that even though Equations (4.1) and (4.2) could have produced dramatically different results (e.g., depending on the choice of Ω_m), the best fit Λ CDM model has parameter values that bring it closest to the $R_h = ct$ Universe. This is the same phenomenon that emerged from fits to the Type Ia SNe data [7], and to the gamma-ray burst Hubble diagram [17], where the distance versus redshift relationship produced by the best fit Λ CDM model appears to be relaxing to that expected in the $R_h = ct$ cosmology.

Though the number of sources used here is still rather small, it is already quite evident from these figures that eventually the catalog of high- z quasars with measured Mg II line-widths and flux densities at 3000 \AA will be large enough to significantly reduce the scatter reflected in the standard deviations listed in Table 3. Much work still needs to be done in assembling a high-quality sample of $z > 6$ quasars for this kind of study, but these

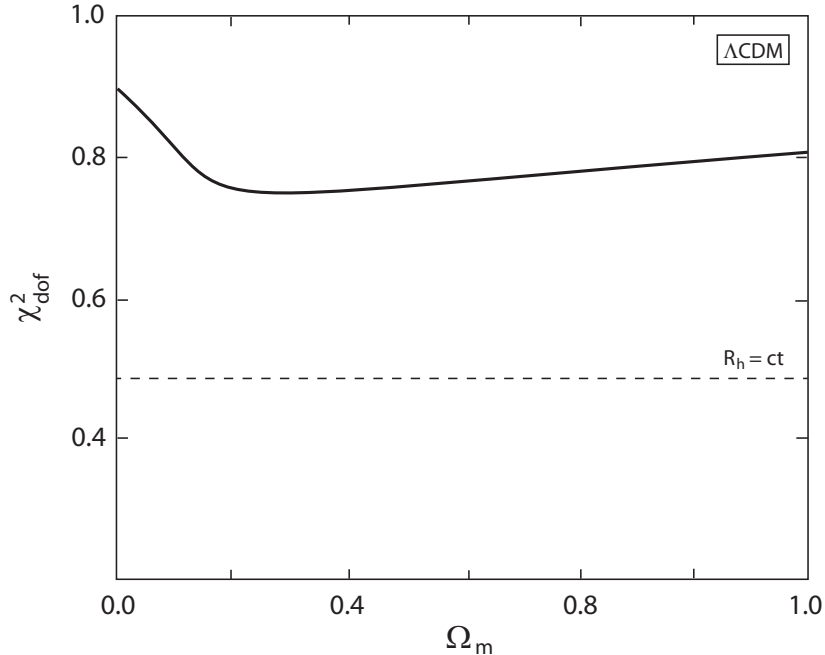


Figure 4. Reduced χ^2 for Λ CDM fits to the data shown in figure 1, as a function of Ω_m . The minimum χ_{dof}^2 is realized for $\Omega_m = 0.27$, which produces a luminosity distance curve over this redshift range essentially identical to that in the $R_h = ct$ Universe (see figure 1). For reference, the dashed line shows the reduced χ_{dof}^2 for the $R_h = ct$ Universe which, however, does not depend on Ω_m .

results already suggest that the effort will be worthwhile. We notice, in particular, that ULAS J1120+0641 (at $z = 7.085$) fits the theoretical curves remarkably well, confirming our suspicion that quasars tend to accrete at a rate closer to the Eddington value the higher their redshift.

The importance of this source in anchoring the fits shown in figure 1 is quite evident, for it provides a significant stretching in the range of sampled redshifts. But suppose that instead of assigning a standard deviation of 0.9 to the highest redshift bin, we use the sample-averaged value of 2.1. How would the fits shown in figure 1 be affected by this change? As it turns out, the optimized parameter values remain the same, though the reduced χ_{dof}^2 's change slightly. For the $R_h = ct$ Universe, we would now have $\chi_{\text{dof}}^2 = 0.44$ (instead of 0.48), while for Λ CDM the corresponding value associated with $\Omega_m = 0.27$ is 0.73 (instead of 0.76). In other words, the reason ULAS J1120+0641 has such a large influence on the results is not only because of its relatively small error bar, but primarily because of its much higher redshift compared to the other sources listed in Table 3.

5 Discussion and Conclusions

In the past decade, over 50 quasars have been discovered at $z > 6$ with the help of dedicated programs, such as the SDSS and CFHQS. Two recent developments have made it possible for us to start thinking about using these powerful sources to construct a Hubble Diagram well beyond the redshift range ($z < 1.8$) accessible to Type Ia SNe, and even GRBs, most of which are expected to be discovered at $0 < z < 6$. High- z quasars therefore offer us a unique

opportunity of studying the expansion of the Universe in its very important early epoch, where there appears to be a paucity of other possible standard candles.

As we have seen, the hypothesis that high- z quasars accrete at close to their Eddington rate and, especially, that their distribution in Eddington factors is the smallest of any redshift range sampled thus far, plus the apparent correlation between the line widths in their broad-line region and their optical/UV luminosity, allows us to use their sample-averaged Eddington luminosity as a standard candle. We have highlighted the inference that, because the actual λ_{Ed} distribution of these sources has an observed finite width (roughly 0.28 dex), it is not possible to use individual sources to construct the HD without introducing some contamination by quasars with $\lambda_{\text{Ed}} > 2$ or $\lambda_{\text{Ed}} < 0.4$. Nonetheless, we have also demonstrated that as long as the Eddington-factor distribution $\phi(\lambda_{\text{Ed}})$ is nearly constant over the redshift range $z \sim 6 - 8$, we can use sample-averaged estimates of the luminosity distance to test competing models. With the procedure we have described in this paper, we expect that an extended high-quality survey will thus permit us to probe the history of the universe over the first 1–2 Gyr of its expansion.

We have also seen how crucial it is to extend the quasar redshift range beyond 7, which is necessary to provide sufficient leverage when fitting theoretical luminosity distances to the data. In this regard, the work we have reported here would not have been feasible without the recent discovery of ULAS J1120+0641 at $z = 7.085$. Quite remarkably, the inferred luminosity distance to this source matches the best-fit curves rather well. This may be somewhat fortuitous, but may also be a confirmation of the expectation that quasars accrete closer to their Eddington rate, the higher their redshift, thus affirming our conclusion that the Eddington-factor distribution $\phi(\lambda_{\text{Ed}})$ probably does remain narrow and constant towards higher redshifts. Clearly, every effort should be expended to acquire additional quasars at $z > 7$.

An interesting alternative proposal to use Active Galactic Nuclei (AGNs) for cosmological distance measurements was made recently [52]. This idea is also based on the observed relationship between the luminosity of type 1 AGNs and the sizes of their broad-line regions (see Eq. 1), but using the actual observed time delay τ between the response of the flux in the broad lines to variations in the luminosity of the central source in order to calculate the radius, R , of the BLR. With this approach, the observable quantity τ/\sqrt{F} , where F is the AGN continuum flux, is then a measure of the luminosity distance to the source.

At least for the foreseeable future, however, this method probably cannot be used to construct the quasar HD at the high redshifts we are considering here. The problem is that extending the catalog to high redshifts requires substantially longer temporal baselines because (1) redshift increases the observed-frame lags due to time dilation effects, and (2) at higher redshifts we observe more luminous AGNs, which have larger BLRs and hence larger rest-frame lags. For example, Watson et al. estimate a $\text{H}\beta$ observed lag of ~ 2 years at $z \sim 2$. The lag reaches close to a decade at $z \sim 2.5$, making this the practical redshift limit for obtaining lags with $\text{H}\beta$. Strong UV lines, such as C IV 1549 Å, can do better because the BLR is ionization-stratified, so these higher excitation lines are emitted closer to the central source. Thus, C IV lags could in principle be measurable for objects up to $z \sim 4$, but almost certainly not beyond $z \sim 5 - 6$. The approach we have described in this paper therefore has the unique potential of extending cosmological distance measurements to redshifts well beyond even this alternative use of high- z AGNs.

The construction of a high- z quasar HD has allowed us to continue our comparison of ΛCDM with the $R_{\text{h}} = ct$ Universe, which has so far been superior to the former in being

able to account for several hitherto inexplicable coincidences and observations that appear to be at odds with the predictions of the standard model. For example, we have recently shown [53] that, whereas Λ CDM cannot explain the implied early appearance of $10^9 M_\odot$ supermassive black holes without invoking anomalously high accretion rates or the creation of exotically massive seeds, neither of which is seen in the local universe, in the $R_h = ct$ Universe, $5 - 20 M_\odot$ seeds produced from the deaths of Pop II and III stars at $z < 15$ could have easily grown to $M \sim 10^9 M_\odot$ by $z \sim 6$, merely by accreting at the standard Eddington rate. The recent observations we have discussed in this paper have compounded the problem for Λ CDM by demonstrating that in fact all of the high- z quasars appear to be accreting at or below this rate, commensurate with the expectations in the $R_h = ct$ cosmology.

In this paper, we have found that both $R_h = ct$ and Λ CDM fit the current catalog of high- z quasars quite well. It is noteworthy that the Λ CDM fit is optimized for the parameter value $\Omega_m = 0.27$, consistent with expectations from the concordance model. As we have demonstrated before [7], this choice of parameters results in a luminosity distance versus redshift relation virtually identical to that of $R_h = ct$ (compare the $\Omega_m = 0.27$ curve in figure 1 with the curve for $R_h = ct$). This appears to be further evidence that the parameters in Λ CDM allow it to relax to the $R_h = ct$ expansion profile when fitting the data.

Having said this, the process of model selection does take into account the number of unrestricted parameters used in the optimization process, and in this regard, the result of our analysis in this paper tends to favor $R_h = ct$ over Λ CDM. In a companion paper [6], we examined how the redshift dependence of the Hubble constant $H(z)$ predicted by the $R_h = ct$ and Λ CDM cosmologies compares with the cosmic chronometer data. These measurements sample a much lower redshift range (typically $z < 2$) [54]. In that work, we discussed at length how one may use state-of-the-art statistical tools to select the model most likely to be correct in accounting for the data. Though we will not reproduce that extensive discussion here, we do point out that to compare the evidence for and against competing models, such as models of the distance–redshift relationship, the use of the Akaike Information Criterion (AIC) is now common in cosmology [55–57]. The AIC can be viewed as an enhanced “goodness of fit” criterion, which extends the usual χ^2 criterion by taking account of the number of parameters in each model.

The AIC provides the relative ranks of two or more competing models, and also a numerical measure of confidence that each model is the best. These confidences are analogous to likelihoods or posterior probabilities in traditional statistical inference, but unlike traditional inference methods, the AIC can be applied to models that are not “nested,” such as we have here. The AIC for the fitted model is given by

$$\text{AIC} = \chi^2 + 2n , \quad (5.1)$$

where n is the number of unknown parameters. Then, a quantitative ranking of models 1 and 2 can be computed as follows. If AIC_α comes from model α , the unnormalized confidence that this model is true is the “Akaike weight” $\exp(-\text{AIC}_\alpha/2)$. Informally, model α has likelihood

$$P(\alpha) = \frac{\exp(-\text{AIC}_\alpha/2)}{\exp(-\text{AIC}_1/2) + \exp(-\text{AIC}_2/2)} \quad (5.2)$$

of being the correct choice. From the analysis we have carried out in this paper, the Akaike Information Criterion has the value $\text{AIC}_1 \approx 4.4$ for $R_h = ct$, compared with $\text{AIC}_2 \approx 8.3$ for Λ CDM. Therefore, the probability of $R_h = ct$ being the correct choice is $\approx 87\%$, while Λ CDM

would be selected with a relative confidence level of only $\approx 13\%$. Two other commonly used model selection criteria are the Kullback Information Criterion (KIC) [58] and the Bayes Information Criterion (BIC) [59], defined as $\text{KIC} = \chi^2 + 3n$ and $\text{BIC} = \chi^2 + (\ln N)n$, where N is the number of measurements. The result of our fitting shows that both the KIC and BIC favor $R_h = ct$ over ΛCDM by a ratio of about 85 – 95% to 5 – 15%. Thus, all three of these statistical tools confirm each other’s outcome—that the high- z quasars reveal a preference for $R_h = ct$ over ΛCDM .

Of course, no one would suggest yet that the probabilities we have calculated here are sufficient on their own to clinch the case for $R_h = ct$, but they do reinforce the conclusion arrived at elsewhere, that this cosmology likely provides the correct expansion history for the Universe, while ΛCDM is a parameter-driven approximation to it.

Even though the Hubble Diagram we have constructed here is limited by relatively large uncertainties (due primarily to the still small sample), the results we have reported in this paper do suggest that high- z quasars may eventually yield information on the luminosity distance at $z > 6$ with sufficient precision for us to carry out a meaningful examination of the Universe’s early expansion history, complementing the highly detailed study already underway (with both Type Ia SNe, GRBs, and cosmic chronometers) at lower redshifts.

Acknowledgments

I am grateful to the many workers who spent an extraordinary amount of effort and time accumulating the data summarized in Tables 1–3. I am also very thankful for the thoughtful and constructive comments of the anonymous referee, resulting in a significantly improved manuscript. I acknowledge Amherst College for its support through a John Woodruff Simpson Lectureship. This work was partially carried out at the Purple Mountain Observatory in Nanjing, China.

References

- [1] Riess, A. G. et al., “Observational Evidence from Supernovae for an Accelerating Universe and a Cosmological Constant,” *AJ*, **116**, 1009 (1998)
- [2] Perlmutter, S. et al., “Discovery of a supernova explosion at half the age of the universe,” *Nature*, **391**, 51 (1998)
- [3] Perlmutter, S. et al., “Measurements of Omega and Lambda from 42 High-Redshift Supernovae,” *ApJ*, **517**, 565 (1999)
- [4] Garnavich, G. et al., “Supernova Limits on the Cosmic Equation of State,” *ApJ*, **509**, 74 (1998)
- [5] Schmidt, B. P. et al., “The High-Z Supernova Search: Measuring Cosmic Deceleration and Global Curvature of the Universe Using Type IA Supernovae,” *ApJ*, **507**, 46 (1998)
- [6] Melia F. & Maier, R., “Cosmic Chronometers in the $R_h = ct$ Universe,” *MNRAS*, **432**, 2669 (2013)
- [7] Melia, F., “Fitting the Union2.1 Supernova Sample with the $R_h = ct$ Universe,” *AJ*, **144**, article id. 110 (2012a)
- [8] Melia, F. & Shevchuk, A., “The $R_h = ct$ Universe,” *MNRAS*, **419**, 2579 (2012)
- [9] Bennett, C. L. et al., “The Microwave Anisotropy Probe Mission,” *ApJ*, **583**, 1 (2003)
- [10] Ade, P.A.R. et al., “Planck 2013 results. XXIII. Isotropy and Statistics of the CMB,” *A&A*, in press, arXiv:1303.5083 (2013)
- [11] Copi, C. J., Huterer, D., Schwarz, D. J. & Starkman, G. D., “No large-angle correlations on the non-Galactic microwave sky,” *MNRAS*, **399**, 295 (2009)
- [12] Melia, F., “The Cosmic Horizon,” *MNRAS*, **382**, 1917 (2007)
- [13] Jimenez, R. & Loeb, A., “Constraining Cosmological Parameters Based on Relative Galaxy Ages,” *ApJ*, **573**, 37 (2002)
- [14] Ghirlanda, G., Ghisellini, G., Lazzati, D. & Firmani, C., “Gamma-Ray Bursts: New Rulers to Measure the Universe,” *ApJ Letters*, **613**, L13 (2004)
- [15] Schaefer, B. E., “The Hubble Diagram to Redshift $z \leq 6$ from 69 Gamma-Ray Bursts,” *ApJ*, **660**, 16 (2007)
- [16] Qi, S. & Lu, T., “Toward Tight Gamma-Ray Burst Luminosity Relations,” *ApJ*, **749**, 99 (2012)
- [17] Wei, J.-J., Wu, X. & Melia, F., “The Gamma-ray Burst Hubble Diagram and its Implications for Cosmology,” *ApJ*, **772**, 43 (2013)
- [18] Willott, C. J. et al., “Eddington-limited Accretion and the Black Hole Mass Function at Redshift 6,” *AJ*, **140**, 546 (2010)
- [19] De Rosa, G., Decarli, R., Walter, F., Fan, X., Jiang, L., Kurk, J., Pasquali, A. & Rix, H. W., “Evidence for Non-evolving Fe II/Mg II Ratios in Rapidly Accreting $z \leq 6$ QSOs,” *ApJ*, **739**, 56 (2011)
- [20] Mortlock, D. J. et al., “A luminous quasar at a redshift of $z = 7.085$,” *Nature*, **474**, 616 (2011)
- [21] Shen, Y. & Kelly, B. C., “The Demographics of Broad-Line Quasars in the Mass-Luminosity Plane. I. Testing FWHM-Based Virial Black Hole Masses,” *ApJ*, **746**, 169 (2012)
- [22] Blandford, R. D. & McKee, C. F., “Reverberation mapping of the emission line regions of Seyfert galaxies and quasars,” *ApJ*, **255**, 419 (1982)
- [23] Kaspi, S., Smith, P. S., Netzer, H., Maoz, D., Jannuzi, B. T. & Givon, U., “Reverberation Measurements for 17 Quasars and the Size-Mass-Luminosity Relations in Active Galactic Nuclei,” *ApJ*, **533**, 631 (2000)

- [24] Bentz, M. C., Peterson, B. M., Netzer, H., Pogge, R. W. & Vestergaard, M., “The Radius-Luminosity Relationship for Active Galactic Nuclei: The Effect of Host-Galaxy Starlight on Luminosity Measurements. II. The Full Sample of Reverberation-Mapped AGNs,” *ApJ*, **697**, 160 (2009)
- [25] Wandel, A., Peterson, B. M. & Malkan, M. A., “Central Masses and Broad-Line Region Sizes of Active Galactic Nuclei. I. Comparing the Photoionization and Reverberation Techniques,” *ApJ*, **526**, 579 (1999)
- [26] Shen, Y., Greene, J. E., Strauss, M. A., Richards, G. T. & Schneider, D. P., “Biases in Virial Black Hole Masses: An SDSS Perspective,” *ApJ*, **680**, 169 (2008)
- [27] Steinhardt, C. L. & Elvis, M., “The quasar mass-luminosity plane - III. Smaller errors on virial mass estimates,” *MNRAS Letters*, **406**, L1 (2010)
- [28] Shen, Y., “The Mass of Quasars,” *Bulletin of the Astronomical Society of India*, **41**, 61 (2013)
- [29] Peterson, B. M., in *IAU Symp. 267, Co-Evolution of Central Black Holes and Galaxies*, ed. B. Peterson, R. Somerville & T. Storchi-Bergmann (Cambridge: Cambridge Univ. Press), 151 (2010)
- [30] Peterson, B. M., “Measuring the Masses of Supermassive Black Holes,” *Space Science Rev.*, in press (2013)
- [31] Vestergaard, M. & Osmer, P. O., “Mass Functions of the Active Black Holes in Distant Quasars from the Large Bright Quasar Survey, the Bright Quasar Survey, and the Color-selected Sample of the SDSS Fall Equatorial Stripe,” *ApJ*, **699**, 800 (2009)
- [32] Schneider, D. et al., “The Sloan Digital Sky Survey Quasar Catalog. III. Third Data Release,” *AJ*, **130**, 367 (2005)
- [33] Richards, G. T. et al., “The Sloan Digital Sky Survey Quasar Survey: Quasar Luminosity Function from Data Release 3,” *AJ*, **131**, 2766 (2006)
- [34] Vestergaard, M., Fan, X., Termoniti, C. A., Osmer, P. O. & Richards, G. T., “Mass Functions of the Active Black Holes in Distant Quasars from the Sloan Digital Sky Survey Data Release 3,” *ApJ Lett.*, **674**, 1 (2008)
- [35] Jiang, L. et al., “Gemini Near-Infrared Spectroscopy of Luminous $z \sim 6$ Quasars: Chemical Abundances, Black Hole Masses, and Mg II Absorption,” *AJ*, **134**, 1150 (2007)
- [36] Kurk, J. D. et al., “Black Hole Masses and Enrichment of $z \sim 6$ SDSS Quasars,” *ApJ*, **669**, 32 (2007)
- [37] Kurk, J. D., Walter, F., Fan, X., Jiang, L., Jester, S., Rix, H. W. & Riechers, D. A., “Near-Infrared Spectroscopy of SDSS J0303 - 0019: A Low-luminosity, High-Eddington-Ratio Quasar at $z \sim 6$,” *ApJ*, **702**, 833 (2009)
- [38] Richards, G. T. et al., “Spectral Energy Distributions and Multiwavelength Selection of Type 1 Quasars,” *ApJS*, **166**, 470 (2006)
- [39] Jiang, L. et al., “Probing the Evolution of Infrared Properties of $z \sim 6$ Quasars: Spitzer Observations,” *AJ*, **132**, 2127 (2006)
- [40] Elvis, M. et al., “Atlas of quasar energy distributions,” *ApJS*, **95**, 1 (1994)
- [41] Dunlop, J. S., McLure, R. J., Kulkula, M. J., Baum, S. A., O’Dea, C. P. & Hughes, D. H., “Quasars, their host galaxies and their central black holes,” *MNRAS*, **340**, 1095 (2003)
- [42] Vanden Berk, D. E. et al., “Spectral Decomposition of Broad-Line AGNs and Host Galaxies,” *AJ*, **131**, 84 (2006)
- [43] Fine, S. et al., “Constraining the quasar population with the broad-line width distribution,” *MNRAS*, **390**, 1413 (2008)

- [44] Shankar, F., Weinberg, D. H. & Miralda-Escudé, J., “Self-Consistent Models of the AGN and Black Hole Populations: Duty Cycles, Accretion Rates, and the Mean Radiative Efficiency,” *ApJ*, **690**, 20 (2009)
- [45] McConnell, N. J., Ma, C.-P., Murphy, J. D., Gebhardt, K., Lauer, T. R., Graham, J. R., Wright, S. A. & Richstone, D. O., “Dynamical Measurements of Black Hole Masses in Four Brightest Cluster Galaxies at 100 Mpc,” *ApJ*, **756**, 179 (2012)
- [46] van den Bosch, R.C.E., Gebhardt, K., Gültekin, K., van de Ven, G., van der Wel, A. & Walsh, J. L., “An Over-massive Black Hole in the Compact Lenticular Galaxy NGC1277,” *Nature*, **491**, 729 (2012)
- [47] Wang, J.-M., Du, P., Valls-Gabaud, D., Hu, C. & Netzer, H., “Super-Eddington Accreting Massive Black holes as Long-Lived Cosmological Standards,” *PRL*, **110**, 081301 (2013)
- [48] Wyithe, J.S.B. & Loeb, A., “Photon trapping enables super-Eddington growth of black hole seeds in galaxies at high redshift,” *MNRAS*, **425**, 2892 (2012)
- [49] Melia, F., *High-Energy Astrophysics* (New York: Princeton University Press) (2009)
- [50] Kollmeier, J. A. et al., “Black Hole Masses and Eddington Ratios at $0.3 < z < 4$,” *ApJ*, **648**, 128 (2006)
- [51] Melia, F. & Abdelqadr, M., “The Cosmological Spacetime,” *IJMP-D*, **18**, 1889 (2009)
- [52] Watson, D., Denney, K. D., Vestergaard, M. & Davis, T. M., “A New Cosmological Distance Measure Using Active Galactic Nuclei,” *ApJ Lett*, **740**, L49 (2011)
- [53] Melia, F., “High- z Quasars in the $R_h = ct$ Universe,” *ApJ*, **764**, 72 (2013)
- [54] Moresco, M., Verde, L., Pozzetti, L., Jimenez, R. & Cimatti A., “New constraints on cosmological parameters and neutrino properties using the expansion rate of the Universe to z 1.75,” *JCAP*, **07**, article id 053 (2012)
- [55] Liddle, A. R., “How many cosmological parameters?” *MNRAS*, **351**, L49 (2004)
- [56] Liddle, A. R., “Information criteria for astrophysical model selection,” *MNRAS*, **377**, L74 (2007)
- [57] Tan, M. Y. J. & Biswas, R., “The reliability of the Akaike information criterion method in cosmological model selection,” *MNRAS*, **419**, 3292 (2012)
- [58] Cavanaugh, J. E., “Criteria for linear model selection based on Kullback’s symmetric divergence,” *Aust. N. Z. J. Stat.*, **46**, 257 (2004)
- [59] Schwarz, G., “Estimating the Dimension of a Model,” *Ann. Statist.*, **6**, 461 (1978)